DESIGN OF AN ENHANCED 1 GeV ELECTRON NEUTRINO BEAM

R.A. ONG *, L. SULAK and R. WATTS

Randall Laboratory, University of Michigan, Ann Arbor, MI 48100, USA

An enhanced ν_e beam would be useful for experiments that have been proposed to investigate the time evolution of a ν_e beam or to test the universality of ν_e and ν_μ interactions. We have performed detailed calculations to maximize the flux of electron neutrinos through a detector while minimizing the more copious muon neutrinos produced at 30 GeV proton accelerators. The ν_e beam is formed from the semi-leptonic decay modes of the neutral kaon. Muon neutrinos generated by decays of charged pions and kaons are suppressed by a dipole sweeping magnet. The ν_e/ν_μ ratio is enhanced from its usual value of $\sim 1/1000$ to a value of $\sim 1/2$, albeit at a low flux. We find with this design a typical flux of $1.5 \times 10^7 \ \nu_e/\text{m}^2$ s. We find that a high magnetic field (≥ 40 kG) is essential to achieve this ν_e/ν_μ enhancement. Although the use of collimators and/or plugs inside the magnet reduces the ν_μ flux, the ν_e flux is also diminished so that there is little beneficial effect on the ν_e/ν_μ ratio. Magnetic focusing horns and quadrupole beams do not enhance the ν_e/ν_μ ratio. The accuracy of the energy dependence of the calculation, as well as the absolute normalization of the fluxes, is determined by a subsidiary calculation of the ν_μ yield from the magnetic horn focused beam at Brookhaven National Laboratory. This calculation is the first to our knowledge to agree well with the ν_μ yield as measured in the BNL seven foot bubble chamber.

1. Introduction

Currently there is a good deal of interest in the possibility of neutrino oscillations and non-zero neutrino masses. This interest stems from the crucial role the neutrino plays in theories which unify the strong and electroweak interactions. Several experiments [1] have studied the time evolution of an accelerator ν_μ beam with reasonably high sensitivity. Because of low ν_e production however (typically one ν_e for every 1000 ν_μ), only a few experiments have obtained information regarding the time evolution of a ν_e beam. This lack of information on accelerator ν_e's is unfortunate since the only published indications of possible oscillations and non-zero neutrino mass occur in the electron neutrino sector. The Savannah River and Bugey reactor experiments have reported the possible disappearance of $\bar{\nu}_e$'s as detected downstream from the reactor source [2]. The CHARM collaboration beam dump experiment at the CERN SPS reports an anomalous prompt $\nu_e : \nu_\mu$ ratio of $1 : 2$ as opposed to the $1 : 1$ ratio expected from the decay of charmed parents [3]. One interpretation of this discrepancy [4] is that the electron neutrinos oscillate into other sectors while travelling from the source to the detectors. The ITEP group has improved their analysis of the end point energy in tritium beta decay and claims

that recent results continue to support a ν_e mass greater than 20 eV [5]. Finally, the apparent deficiency of the solar ν_e's as seen in the Homestake Gold Mine experiment experiment could be interpreted as a result of neutrino oscillations [6].

Phenomenologically, neutrino oscillations are characterized in terms of the evolution in proper time of a massive neutrino. In convenient units this is L/p where L is the neutrino flight path and p is the neutrino momentum. Typically, reactor experiments have explored the region of L/p around 10 m/5 MeV = 2 km/GeV, while the CERN SPS experiments have looked at the region around 900 m/25 GeV = 0.04 km/GeV [7]. These regions in L/p correspond to possible mass differences between neutrino eigenstates of 1 and 50 eV respectively. In examining these regions, however, both reactor and accelerator based experiments have been hampered by systematic problems. For the reactors, problems center around the scarcity of ν_e's and the knowledge of the energy dependence of the neutrino flux; for the beam dump experiments, problems involve the unknown production mechanism of the ν_e's and the low ν_e/ν_μ ratio.

Thus it appears that a neutrino oscillation experiment capable of exploring a large range of L/p and optimized to search for oscillatory behavior of the ν_e sector is desirable. Certainly, the experiment should cover the region of phase space delineated by the recent indications of possible effects ($L/p = 10^{-2}$ to 1 km/GeV), and be sensitive to oscillation effects at the

---

5% level or better, the level expected if neutrino mixing angles are comparable to quark mixing angles between the first two generations. To date there have been no copious accelerator ν_e sources available for such a study, and certainly no ν_e sources with low contamination of ν_μ's.

For a ν_e source, the 30 GeV proton accelerators have clear advantages over alternative neutrino sources [8]. Since they accelerate the highest flux of protons above kaon production threshold [9], the 30 GeV proton machines have the potential for producing the largest number of ν_e's. Furthermore, the neutrino energy range (0.5–4 GeV) and accessible detector distances (40 m–1.5 km) naturally yield the desired L/p range. Although high fluxes of low energy ν_e's from muon decay are available at pion factories, they are limited in several ways. The 53 MeV maximum neutrino energy places an upper limit on the sensitivity to neutrino mass differences for typical detector distances. A lower limit at LAMPF comes from the 6% duty cycle which leads to an unavoidable cosmic ray background at large flight paths (where the event rate is necessarily low). Furthermore, the ν_e's from muons decaying at rest are produced isotropically. Thus one lacks the intensification gained by the Lorentz focusing inherent in neutrino beams produced by decay in flight. Going to higher energies at Fermilab or the SPS at CERN turns out not to be advantageous. Neutrinos produced at these facilities are too high in energy to achieve adequate sensitivity to small neutrino mass differences. In addition, neutrino production processes above charm threshold are not well understood thus preventing unambiguous interpretations of deviations from nominal neutrino event rates.

The most favorable conditions for production of a ν_e beam to be used for oscillation studies therefore appear to be at the 30 GeV proton accelerators, the Brookhaven AGS or the CERN PS. Such studies have been suggested [10,11]. To determine the feasibility of the proposed experiments, an understanding of the ν_e flux, both in energy dependence and in absolute magnitude, is needed as a function of distance from the production region. In addition, suppression of ν_μ production must be optimized and the remaining ν_μ background evaluated. To address these issues, we have performed a detailed computer simulation, incorporating all known aspects of the production and propagation of a neutrino beam.

We first outline the structure of the simulation. We then test it by comparing our generated ν_μ spectrum with an experimentally determined one. We conclude with an explicit example of a possible design for a ν_e beam at BNL, the prediction of the ν_e energy spectrum, and an evaluation of the accompanying ν_μ background.

2. General description of the ν_e beam

The salient characteristics of possible ν_e beams at BNL and at CERN are quite similar. For concreteness, we pursue the parameters of the suggestions initially made by the authors [10]. Fig. 1 shows the first 100 m of the beamline. Incoming 28 GeV protons from the AGS strike a pencil target producing a secondary beam composed primarily of pions and kaons. A list of the simulated secondary particles, along with their decay products and branching ratios, is given in table 1. Other particles and decay modes are assumed to be insignificant. After production, most charged particles are swept out of the beam by the strong dipole sweeping magnet surrounding the target. The remaining particles are then allowed to decay while they travel downstream to the iron muon shield. The shield is assumed to absorb everything but the neutrinos. They pass into the detector and are counted. The neutrino detector consists of several massive water Cherenkov modules judiciously spaced along the neutrino beam line. Fig. 1 shows the location of the first detector module 90 m from the target. Further detector modules are located at 250, 500 and 1500 m from the target. For the purposes of this study we will determine the neutrino flux into a detector of three meters in diameter placed directly behind the iron shield.

The electron neutrino beam is generated primarily from the semi-leptonic decays of K_L^0's. In principle, one would also like to use K^+ semi-leptonic decays, but there appears to be no way to suppress the dominant background of ν_μ's from π^+ decay without also suppressing the ν_e's from K^+ decay. The major source of background in the detector is due to ν_μ events which masquerade as ν_e events. To cut down the number of ν_μ's entering the detector and thus increase the signal to noise ratio, a magnet is used to sweep out the charged pions and kaons that give rise to the majority of ν_μ's. The residual ν_μ's which arrive at the detector result from secondaries that decay before being sufficiently bent out of the beam and from the products of K_L^0 and Λ^0 decay.
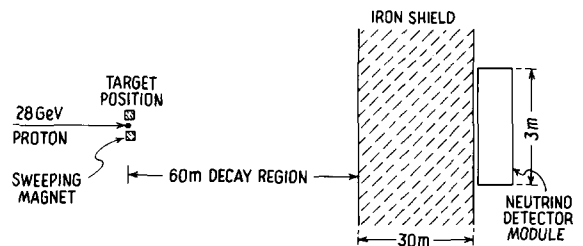

Fig. 1. Layout of first 100 m of BNL ν_e beam line.

Table 1
Decay products and branching ratios

Secondary	Decay mode	Branching ratio
π^+	$\nu_\mu \mu^+$	1.00
π^-	$\bar{\nu}_\mu \mu^-$	1.00
K^+	$\nu_\mu \mu^+$	0.64
	$\pi^+ \pi^0$	0.21
	$\pi^+ \pi^+ \pi^-$	0.056
K^-	$\bar{\nu}_\mu \mu^-$	0.64
	$\pi^- \pi^0$	0.21
	$\pi^+ \pi^- \pi^-$	0.056
K^0_S	$\pi^+ \pi^-$	0.69
K^0_L	$\pi^+ e^- \bar{\nu}_e$	0.19
	$\pi^- e^+ \nu_e$	0.19
	$\pi^+ \mu^- \bar{\nu}_\mu$	0.14
	$\pi^- \mu^+ \nu_\mu$	0.14
	$\pi^+ \pi^- \pi^0$	0.12
μ^+	$e^+ \bar{\nu}_\mu \nu_e$	0.19
μ^-	$e^- \nu_\mu \bar{\nu}_e$	0.99
Λ^0	$p \pi^-$	0.64

3. Details of the ν_e and ν_μ flux simulation

The simulation was written in FORTRAN for use on a DEC VAX-780 computer. The significant parameters used in the simulation are listed in tables 2 and 3. Described below are the important features of the simulation.

The incident proton beam is modeled as a normally incident, radially symmetric Gaussian distribution with

Table 2
Parameters of BNL ν_μ beam line with focusing horn

Proton momentum	27.8 GeV/c
Target:	
length	52.5 cm
radius	0.3175 cm
material	sapphire (Al$_2$O$_3$) [a]
density	3.987 g/cm^3
Focusing device: BNL neutrino horn	
current	270 kA
Decay tunnel:	
length	53.9 m
radius	70 cm (first 10 m)
	1.5 m (remaining length)
Iron shield:	
length	31.7 m
Detector:	
radius	56.4 cm
center	9.77 m after iron shield

[a] Sapphire target is modeled as beryllium since the Eichten data shows little difference between Al and Be.

a spatial $\sigma_r = 1.4$ mm, and a Gaussian angular distribution with $\sigma_\theta = 2.5$ mrad [12]. The beam is exponentially absorbed in the target. The interaction vertex is randomly picked according to these constraints. Typically, 20% of the incident protons do not interact with the target and are ignored by the program. The target is assumed to be beryllium, with an absorption length of 36.7 cm. Beryllium is chosen because it produces the highest kaon yield per target interaction [13]. Subsequent interactions of each proton with the target are ignored.

Secondary pions and kaons resulting from p–Be collisions are generated by using the production spectra measured by Eichten et al. at CERN [13]. To obtain an analytic expression for the production spectra, a modified version of the 1967 Sanford–Wang parametrization is used as an interpolating tool [14]:

$$\frac{d^2 N}{d\Omega dP}\bigg|_{\text{Sanford-Wang}} (\#/\text{SrGeV}/c) = C_1 P^{C_2}\left(1 - \frac{P}{P_i}\right)$$

$$\times \exp\left[\frac{-C_3 P^{C_4}}{P^{C_5}} - C_6 \theta\left(P - C_7 P_i \cos^{C_8}\theta\right)\right].$$

where: P = momentum of secondary particle,
θ = the production angle of the secondary,
P_i = momentum of incident proton, and
$C_1 - C_8$ = fitting coefficients listed in table 4.
This parametrization is modified so that the results match the experimental data of Eichten et al. at 24 GeV/c. The modification for the π^+, π^-, and K^+

Table 3
Parameters of BNL ν_e enriched beam line

Proton momentum	28 GeV/c
Target:	
length	75 cm
radius	0.25 cm
material	Be
density	1.848 g/cm^3
Magnet: BNL 18 D 72 dipole	
length	72''
gap	6'' × 19''
field	22 kG
Decay tunnel:	
length	60 m
radius	2 m
Iron shield:	
length	30 m
Model detector:	
radius	1.5 m
location	following iron shield
fiducial mass (H$_2$O)	1 kt

Table 4
Coefficients for modified Sanford–Wang parametrization

Secondary	C_1	C_2	C_3	C_4	C_5	C_6	C_7	C_8
π^+	1.092	0.6458	4.046	1.625	1.656	5.029	0.1722	82.65
π^-	0.821	0.5271	3.956	1.731	1.617	4.735	0.1984	88.75
K^+	0.059	0.6916	3.744	4.520	4.190	4.928	0.1922	50.28

secondaries is

$$\frac{d^2N}{d\Omega\,dP} = \frac{d^2N}{d\Omega\,dP}\bigg|_{\text{Sanford-Wang}}$$

$$\times F(P)(1.0 + CP)\left[1 + A(\theta - \theta_0) + B(\theta - \theta_0)^2\right],$$

where the coefficients A, B and C are given in table 5, and the function $F(P)$ is given in table 6. Although the modified production spectra fit the Eichten data well, we fix the fit at $\theta_0 = 17$ mrad, the average acceptance of a typical detector. The K^- production spectra are derived from the K^+ spectra by the following empirical fit:

$$\frac{d^2N}{d\Omega\,dP}(K^-) = \begin{cases} \dfrac{d^2N}{d\Omega\,dP}(K^+)\dfrac{F(P)}{2.7}, \\ \qquad \text{for } P < 4 \text{ GeV}/c, \\ \dfrac{d^2N}{d\Omega\,dp}(K^+)\dfrac{F(P)}{\left[2.7 + 0.134(P - 4.0)^2\right]}, \\ \qquad \text{for } P \geq 4 \text{ GeV}/c. \end{cases}$$

Figs. 2 and 3 compare generated π^+ and K^+ spectra against Eichten's data for secondary momenta of 5 and 8 GeV/c and for production angles from 0 to 100 mrad.

Table 5
Coefficients for modified Sanford–Wang parametrization

Secondary	A	B	C
π^+	-1.0×10^{-3}	1.0×10^{-6}	0.45
π^-	-5.0×10^{-3}	1.5×10^{-5}	0.0
K^+	2.0×10^{-4}	-2.3×10^{-6}	4.0

Table 6
Coefficients for modified Sanford–Wang parametrization

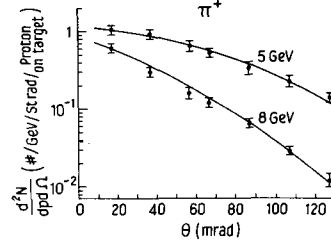| Secondary	$F(p)$	
π^+	$0.1424p^2\,e^{-0.1809p}$	$p > 4$ GeV/c
	$0.5985p$	$p \leq 4$ GeV/c
π^-	$0.4443p\,e^{-0.0713p}$	$p > 4$ GeV/c
	$0.7044p$	$p \leq 4$ GeV/c
K^+	1.273	$p > 4$ GeV/c
	$0.0155p\,e^{-0.0713p}$	$p \leq 4$ GeV/c
K^-	$0.2355p$	$p < 4$ GeV/c

Fig. 2. Angular production spectra comparison for π^+ at 5 GeV/c and at 8 GeV/c. Solid line is interpolated spectrum described in text while points with error bars are data of Eichten et al.

Comparisons at other momenta and for π^- and K^- secondaries show similar good agreement to the Eichten data. The bulk of the detected neutrino signal comes from these regions in the spectra. Note that the parameterization gives results which do not diverge at low momenta and at zero angle where no data exists. To obtain the K_L^0 spectra, isospin invariance is invoked and the average of the K^+ and K^- spectra is taken at the desired momentum and angle. For each momentum and polar angle generated, a random azimuthal angle is chosen.

Secondaries produced in the target are propagated through the target in 1 cm increments. At each step the particle suffers dE/dx ionization loss and bending in the magnetic field. Since the typical multiple Coulomb scattering angle is much less than the production angle, it is ignored. Secondaries that are found to have been scattered inelastically are assumed to be completely removed from the system, along with any tertiary particles they may create. Inelastic scattering supresses the
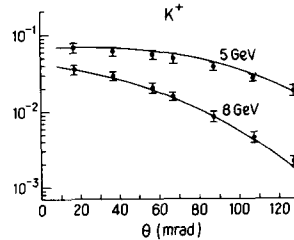

Fig. 3. Angular production spectra comparison for K^+ at 5 GeV/c and at 8 GeV/c.

ν_e flux from K_L^0 decays, since the majority of the ν_e's that arrive at the detector come from K_L^0's that travel the entire length of the target at low production angles (< 30 mrad).

In addition to the target, we consider absorption of particles in the magnet system, the decay tunnel and the iron shield. Because the magnetic field region depends on the experimental configuration, a discussion of absorption by each configuration is presented below. Absorption at the decay tunnel walls is assumed to be total, i.e. the particle and all potential products of the absorptive interaction are removed from consideration. Likewise, all particles other than neutrinos are totally absorbed by the iron shield.

All decays are assumed to be isotropic in the center of mass except for the semi-leptonic neutral kaon decays and the $\mu \rightarrow \nu_\mu \nu_e e$ decay. The kaon decays are calculated according to the distributions given by the V–A theory and observed Dalitz plot data [15]. The production of the two neutrinos from muon decay assumes a V–A interaction.

4. Comparison of simulation with existing ν_μ spectra

To check the simulation described above, we test its predictions against known data. In particular, to determine the absolute normalization of the flux generated by the simulation, the parameters of the program were modified to simulate the muon neutrino data taken by Murtagh et al., in the Brookhaven seven foot bubble chamber [16]. The physical parameters of this beam line are given in table 2 [17]. The focusing system of the Brookhaven neutrino beam line is a double magnetic horn. It is a set of concentric conductors that focus charged pions and kaons, and hence increase the $\nu_\mu (\bar{\nu}_\mu)$ flux. The complex structure of the conductors is modeled as a set of cylinders and cones enclosing a magnetic field falling off as $1/r$. Because of the shape of the horn, an analytic solution for particle trajectories is not attempted. Instead, the particles are stepped through the system in small increments.

Fig. 4 shows the transfer curves for 5 and 7 GeV π^+'s created on axis approximately halfway down the length of the target. The cusps in the figures are the result of discontinuities in the magnet geometry. To obtain these curves, the particles are propagated through the horn in 1 mm steps. However, this procedure requires a large amount of computing time. A coarser grid is used to generate many events: the particle is moved in steps of 1 cm for a radial distance less than 6 cm, 5 cm for a radial distance less than 18 cm, and 10 cm otherwise. In this procedure, the field inhomogeneity across a single step is always less than 15% and the transmission curves are in good agreement with fig. 4. As can be seen
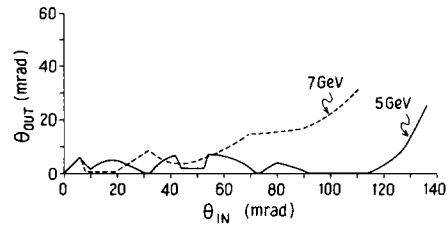

Fig. 4. Transfer curves for BNL horn magnet system. Curves are for 5 and 7 GeV/c π^+'s created 25 cm into the target.

from this figure, the magnet system is excellent at focusing particles up to 100 mrad, depending on the momentum. Fig. 5 shows the trajectories of 5 GeV π^+'s created at several positions and production angles in the target. As an example, a π^+ created 25 cm into the target with an angle of 50 mrad is almost perfectly focused at the end of 2 m. In fact, all π^+'s created with an angle less than 137 mrad are focused into the 34 mrad acceptance of the decay tunnel. With the magnetic horn set to focus positively charged particles and defocus negative ones, the typical focusing factor for π's is 23.9 and the typical defocusing factor is 5.0. These factors are calculated for those neutrinos that make it into a 1.1 m diameter detector located 90 m downstream from the target, a reasonable representation of the BNL seven foot chamber.

Absorption of particles by the horn system is taken into account as the particles are transported through the magnets. The inner and outer conductors of each horn are taken to be 1/8 inch thick aluminum and the first horn has a 7/8 inch thick aluminum end plate. Absorption is assumed to be total. In addition, the target is cooled by a water jacket between it and the inner
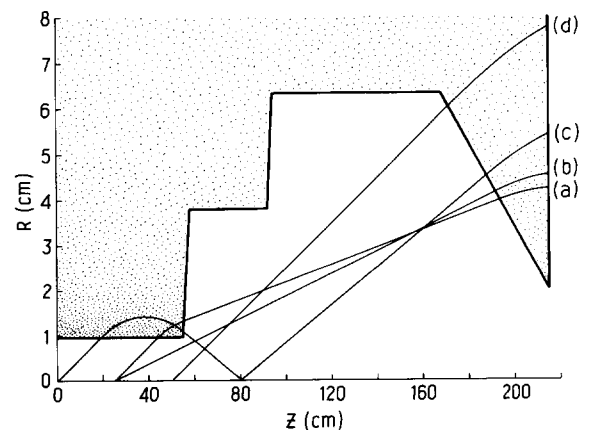

Fig. 5. Trajectories of a 5 GeV π^+ through the first BNL horn magnet. (a) $\theta = 50$ mrad created at $z = 25$ cm. (b) $\theta = 25$ mrad, $z = 25$ cm. (c) $\theta = 40$ mrad, $z = 0$ cm. (d) $\theta = 75$ mrad, $z = 25$ cm.

conductor of the first horn segment. The effects of absorption by this water are not included in the simulation. Similarly, absorption by additional flanges, bolts, etc. are ignored.

Fig. 6 displays the muon neutrino flux through the BNL seven foot chamber for neutrinos from π^+ and K^+ secondaries as calculated by the simulation. Error bars in this figure and in the following ones are statistical only. The sum of these fluxes is normalized with the observed ν_μ flux in fig. 7. The observed flux is obtained by identifying quasi-elastic neutrino events in the fiducial volume of the bubble chamber and assuming that the neutrino flux is uniform across the diameter of the chamber. Also displayed in this figure is the flux as calculated by Tso [18]. Absolute neutrino flux calculations have traditionally been up to an order of magnitude higher than observed fluxes due to the inability to account for targeting efficiency, beam monitoring etc. The results of our simulation are a factor of 3.6 higher than the BNL data. This normalization factor is included in all subsequent calculations. The simulation shape and the BNL data agree well in all regions, with excellent agreement from 0.5 to 2.0 GeV. Our calculations fit the data well at high energy, where the Tso spectrum is a factor of two too high. Note that the contributions to the ν_μ flux from the decay of K^0 secondaries and from the decay of tertiary muons are negligible.
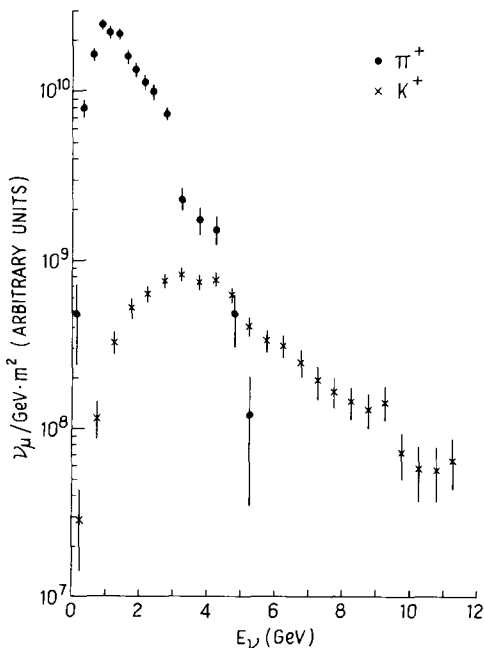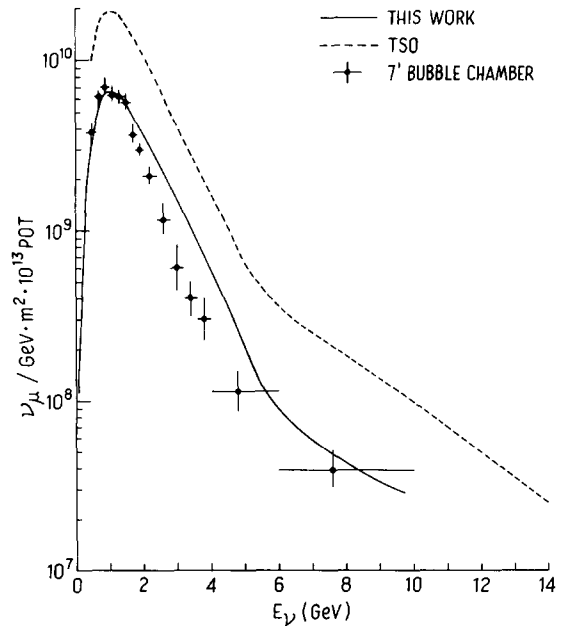
There are other predictions of the BNL muon neu-

Fig. 7. Plot of BNL ν_μ fluxes.

trino flux [19]. Such predictions either peak at a higher energy than does the data, have a larger flux at higher energy, or have both problems. To our knowledge, the simulation of this paper is the best fit to date of the Brookhaven ν_μ flux.

5. Design of an enriched ν_e beam

The main goal of the ν_e beam design is to minimize the number of ν_μ's entering the detector by sweeping charged pions and kaons out of the beam before they decay. In this way, the ν_e/ν_μ ratio can be increased by about two orders of magnitude over a configuration without a sweeping magnet. The final design parameters are listed in table 3. The length of the target is adjusted to maximize ν_e's from kaon decay at the first proposed detector position. The entire target is placed inside a magnetic field to sweep as many charged secondaries out of the beam as possible.

We modeled a 18 D 72 dipole magnet with a field strength of 22 kG [20]. Because of the large amount of iron surrounding the gap of the magnet (at least one absorption length in every direction) absorption of secondaries by the magnet is assumed to be total.

Because collimation of secondary beams had been used in previous neutral particle experiments, collimation was attempted in this design. However, as figs. 2 and 3 show, pions are generally produced with less transverse momentum that kaons. Collimation stops more kaons than pions, decreasing the ν_e/ν_μ ratio.

Fig. 6. Unnormalized components of the simulated ν_μ BNL beam. Error bars in this and all subsequent figures are statistical only.

In another attempt at increasing the ν_e/ν_μ ratio by selectively absorbing pions over kaons, a tungsten plug was inserted directly after the target. This also decreased the ratio. Only the kaons produced very forwardly yield neutrinos at the detector. The plug in the magnet then stopped these kaons before they decayed. Few pions were stopped since the large majority of them had already been swept out of the plug's path by the magnetic field.

The detector modeled consists of several modules of Cherenkov ring-imaging water calorimeters [10]. Each module of the detector consists of a fiducial volume of 1 kt of water viewed by photomultiplier tubes. The first detector is located after the 30 m muon shield at a distance approximately 90 m downstream from the target.

The production angle for pions (kaons) which decay into neutrinos above 1 GeV in energy at the detector is 40 (100) mrad. By comparison, the angular acceptance of the exit aperture of the dipole magnet from the center of the target is 105 mrad, and that of the midpoint of the decay tunnel from the center of the target is 35 mrad.

The predicted neutrino spectra for this configuration are shown in figs. 8 and 9. Fig. 8 gives the ν_e component of the flux through the detector from K_{e3}^0 decays, while fig. 9 gives a breakdown of the different ν_μ contributions according to parent secondary. Although the flux from pion decay has been suppressed by the sweeping magnet, it still remains the largest source of ν_μ contamination in the ν_e beam. We estimate the contamination of
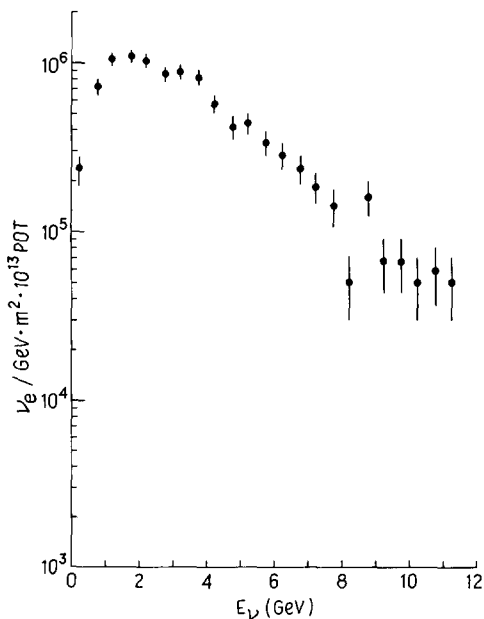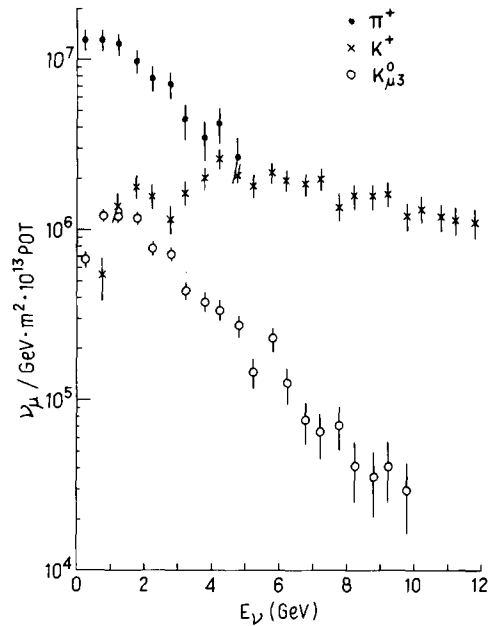

Fig. 9. Plot of predicted ν_μ flux obtained using parameters of table 3 and broken down into contributing components.

ν_μ's from Λ^0 decay to be less than 5% of that from pion and kaon decay. Integrating the curves in figs. 8 and 9, we obtain a ν_e/ν_μ ratio of 1/13.4. One can take advantage of the ν_e spectrum peak at ~ 1 GeV and the rapidly falling ν_μ spectrum. An energy cut at $E_\nu \geq 1$ GeV improves the ν_e/ν_μ ratio to 1/11.6, while maintaining 90% of the ν_e flux. Cutting at an energy of 1.5 GeV gives only a marginal increase to 1/11.3 decreasing the ν_e flux to 80% of its original value. The fluxes obtained with these energy cuts and the net ν_e/ν_μ ratios are listed in table 7. Making the 1 GeV energy cut yields a flux of 2.6×10^{14} ν_e's through the closest 3 m detector for 8.4×10^{19} protons on target, a four month run.

Changing the field strength in the sweeping magnet and the length of the magnet strongly affects the ν_e/ν_μ ratio. This effect is shown in table 7. Doubling the field

Fig. 8. Plot of predicted ν_e flux obtained using the physical parameters of table 3 and normalised to data of Murtagh et al.

Table 7
ν_e fluxes and ν_e/ν_μ ratios for the enriched ν_e beam

Magnetic field	Energy cut	ν_e flux [a] ($\#/m^2$ s)	ν_e/ν_μ ratio
22 kG, 72 in.	none	3.86×10^6	1/13.4
	>1 GeV	3.47×10^6	1/11.6
	>1.5 GeV	3.09×10^6	1/11.3
44 kG, 72 in.	>1 GeV	3.47×10^6	1/2.3
22 kG, 144 in.	>1 GeV	2.88×10^6	1/5.1
44 kG, 144 in.	>1 GeV	2.88×10^6	1/2.0

[a] Flux calculated in a 20 mrad detector at 90 m from the decay point.

strength from 22 to 44 kG increases the ν_e/ν_μ ratio to 1/2.3 for a neutrino energy above 1 GeV. Doubling the magnet length from six feet to twelve feet gives a ν_e/ν_μ ratio of 1/5.1. The ν_e flux is reduced to 83% of the flux with a six foot magnet due to the smaller effective aperture of the longer magnet. By doubling both the magnet field strength and length we obtain a ν_e/ν_μ ratio of 1/2.0 for neutrinos above 1 GeV in energy.

6. Discussion and conclusions

Given the design parameters in table 3 for a ν_e beam line, this design predicts 2.6×10^{14} ν_e's through a 3 m detector in four months, corresponding to a ν_e flux of 3.5×10^6 $\nu_e/m^2 s$. Recent results from proton decay experiments with detectors similar to the one proposed here indicate a typical $\nu_\mu : \nu_e$ rejection ratio of 20 : 1 [21]. Adopting this rejection ratio as a guideline, the design parameters in table 3 predict a neutrino interaction signal to background of ~ 2 : 1 in the detector. Reasonable event rates follow for a sufficiently large detector. The rates are significantly improved by the proposed increase in the BNL AGS proton yield from 2×10^{13} protons per pulse to 1×10^{14} protons per pulse [22]. With a marked increase in the primary proton yield we can also consider a longer and higher strength magnetic field while maintaining an acceptable event rate. Given a 44 kG sweeping manget twelve feet long, and five times the proton flux from the AGS, we calculate 1.1×10^{15} ν_e's through the first detector module in four months. This rate corresponds to a ν_e flux of 1.5×10^7 $\nu_e/m^2 s$ with a ν_e to ν_μ ratio of 10 : 1 and a neutrino event rate of 700/d.

In conclusion, this study has shown that an experiment dedicated to the study of the time evolution of an electron neutrino beam is feasible using existing technology at a 30 GeV proton machine. Good agreement has been obtained between this simulation and the ν_μ spectra measured in the Brookhaven neutrino beam line. This agreement is, to our knowledge, a unique result.

We thank R. Bionta for his contributions to this work. One of the authors (R.A.O.) would like to acknowledge the use of SLAC computers in preparing this work, the help of C. Wendt in reading the manuscript, and the understanding of Prof. J. Jaros.

References

[1] H. Meyer et al. (CDHS Collaboration), Proc. Int. Europhysics Conf. on High Energy Physics '83, Brighton, England, eds., J. Guy and C. Costain, Rutherford Lab, Chilton England (1983) p. 393; W.H. Smith et al. (CCFR Collaboration), ibid., p. 395.

[2] F. Reines, H. Sobel and E. Pasierb, Phys. Rev. Lett. 45 (1980) 1307; Cavaignac et al., LAPP Exp-84-03 (May 1984).

[3] Bergsma et al. (CHARM Collaboration), CERN-EP/84-36 (1984).

[4] A. De Rujula et al., Nucl. Phys. B168 (1980) 54; V. Barger et al., J. Phys. G6 (1980) L165.

[5] Lubimov et al., Proc. HEP '83, p. 386; also Phys. Lett. 94B (1980) 266.

[6] T.B. Cleveland, R. Davis Jr. and J.K. Rowly, Proc. Neutrino Oscillations Workshop (1981) BNL 51380, p. 1.

[7] Recent inclusive ν_μ measurements from the CDHS experiment at CERN over a range of L/p from 0.3 km/GeV to 0.04 km/GeV.

[8] H. Chen, Proc. of ν Oscillation Workshop (1981) p. 217.

[9] L.C. Teng, 1976 Summer Study on Kaon Factories, BNL 50579, p. 189.

[10] L. Sulak et al., Proc. of ν Oscillation Workshop (1981) p. 189.

[11] W. Lee et al., ibid., p. 171.

[12] The parameters presented in the text are a good representation of the extracted proton beam in the U-line of the AGS, just upstream of the present neutrino target. G. Smith, private communication.

[13] T. Eichten et al., Nucl. Phys. B44 (1972) 333.

[14] J.R. Sanford and C.L. Wang, Brookhaven Internal Report, JRS/CLW-1.2 (1967). A later report exists, but we chose the original parametrization since this version fits the angular distribution of the Eichten data better.

[15] L. Jauneau, Methods of Subnuclear Physics, vol. 3, ed., M. Nikolic (New York, 1969) p. 134.

[16] M. Murtagh, private communications.

[17] G. Smith, private communication.

[18] W. Lee et al., Proc. Int. Neutrino Conf., Aachen, Germany, ed., H. Faïssner, H. Reithler and P. Zerwas (1976) p. 320.

[19] For example, C. Baltay and C.L. Wang, private communications. Also Blietschau et al., Nucl. Phys. B133 (1976) 205; Nucl. Phys. B144 (1976) 189 have fluxes calculated for the CERN wide band neutrino beam. These fluxes may be scaled to the Brookhaven parameters but the same reservations made in the text also apply.

[20] K. Raychaudhuri et al., Phys. Lett. 90B (1980) 319.

[21] M. Koshiba et al. (Kamioka Proton Decay Expt), Proc. 23rd Int. Conf. on High Energy Physics, Leipzig, DDR.

[22] B. Palmer, private communication.